ELSEVIER

Journal of Power Sources 113 (2003) 414–421

JOURNAL OF POWER SOURCES

www.elsevier.com/locate/jpowsour

Simultaneous real-time measurements of potential and high-frequency resistance of a lab cell

F. Huet[a,*], R.P. Nogueira[a,b], L. Torcheux[c], P. Lailler[c]

[a]*UPR15 du CNRS "Physique des Liquides et Electrochimie", Université Pierre et Marie Curie, 4 place Jussieu, 75252 Paris Cedex 05, France*

[b]*Laboratório de Corrosão, PEMM/COPPE/UFRJ, C.P. 68505, CEP 21945-970, Rio de Janeiro, RJ, Brazil*

[c]*Compagnie Européenne d'Accumulateurs (CEAC), 5/7 allée des Pierres Mayettes, 92636 Gennevilliers, France*

Abstract

Simultaneous measurements of the potential and high-frequency resistance, R_{HF}, of a lead-acid battery cell of 1200 Ah capacity used in photovoltaic applications have been carried out during the charge and discharge of the cell, owing to an original experimental set-up devised in the laboratory providing real-time analog signals. It was shown that R_{HF} depended on the state-of-charge in a non-linear way, with a significant increase at low state-of-charge. In complementary measurements on cells of smaller capacities (45 Ah), it was observed that the final value of R_{HF} after a complete discharge was higher for a low discharge rate. The R_{HF} variations were explained by the blocking effect of insulating $PbSO_4$ crystals whose morphology and size depend on both state-of-charge and (dis)charge rate. It was also shown that the resistivity of the bulk electrolyte, measured above the plates, had no influence on the R_{HF} value.

Keywords: Lead-acid battery; High-frequency resistance; Internal resistance; Electrochemical impedance; State-of-charge; State-of-health

1. Introduction

The relationship between electric or electrochemical parameters and the state-of-charge (SOC) or the state-of-health (SOH) of lead-acid batteries (LAB) has been widely investigated over the last two decades with a particular interest devoted to ac techniques such as the electrochemical impedance. Reviews on the applicability of impedance measurements as a test of SOC or SOH of LAB have been performed recently [1,2]. Among the various parameters that can be defined from an impedance diagram measured on a wide frequency range, the high-frequency resistance R_{HF} (also called internal resistance and related to the conductance $1/R_{HF}$), has been proposed by Yahchouchi [3] to be a possible indication of the SOH of a LAB cell. Its sensitivity to temperature variations being low, it has been measured since 1992 in large-scale field experiments under the impulse of impedance/conductance tester manufacturers [4,5] for assessing its performance to monitor the SOH of batteries in floating conditions.

Because of the complex behavior of LAB, the accurate estimation of the actual SOH or SOC of LAB remains a matter of major concern. Several methods have been proposed [6,7]. Among those based on impedance spectroscopy, the measurement of R_{HF} is still the subject of investigations. While all authors admit that high values of R_{HF} detect gross defects in bad LAB cells, it is sometimes considered that R_{HF} cannot provide more information because of the dependence of R_{HF} on the type of battery that precludes generalization of the trend given by one type of battery to other batteries [8], or the dispersion of the R_{HF} values for new cells [9], or because of the use of inadequate methods for connecting the cables onto the battery terminals [10]. For this reason, other parameters of the electrochemical impedance, such as the low-frequency resistance or the double layer capacity, which requires measurements of galvanostatic discharge transients [11], of voltage responses to a sudden load application [12], or of electrochemical impedances at several frequencies [13], have been proposed for SOC or SOH monitoring. On the contrary, other authors claim that it is possible to (i) estimate the residual capacity of batteries in uninterruptible power supply systems [14] or of photovoltaic LAB of high capacity [15], or (ii) identify the failure mechanism of LAB (positive plate deterioration or dry-out [16], active material resistance increase [17,18]). On-line battery testings for degradation estimation from R_{HF} measurements

* Corresponding author. Tel.: +33-1-4427-4136; fax: +33-1-4427-4074.
E-mail address: frh@ccr.jussieu.fr (F. Huet).

0378-7753/02/$ – see front matter
PII: S0378-7753(02)00557-8

have even been reported in telecommunication equipments [19,20].

Even if the current knowledge effectively points out the existence of some correlation between SOC and R_{HF}, much remains to be done to explain the origin of the R_{HF} changes with SOC. This paper is aimed at investigating the real-time evolutions of R_{HF} and of the voltage, V, at the terminals of the cell, during the charge and discharge of a 1200 Ah LAB cell used in photovoltaic applications in order to clarify the possible reasons of the R_{HF} changes and evaluate the feasibility of performing state-of-charge diagnostics. Complementary experiments have also been carried out on LAB cells of 45 Ah to study the influence of the charging or discharging rate on the R_{HF} values.

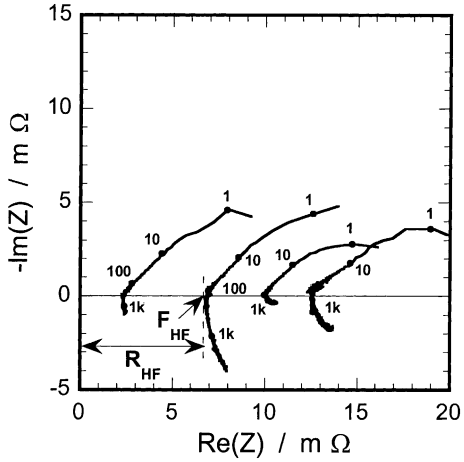

Fig. 2. Nyquist diagrams of the impedance of a 45 Ah LAB cell at rest with different cable connectors and tightening pressures (frequencies in Hz).

2. Experimental

The experimental set-up for the real-time measurement of V and R_{HF} is schematically depicted in Fig. 1. A specific electronic device processed the voltage response of the LAB cell (1200 Ah–2 V, CEAC-Exide, Solar, tubular technology) to a high-frequency current perturbation supplied by the galvanostat. In order to ensure that the response of the interface was effectively related to R_{HF}, the frequency of this current perturbation was chosen as close as possible to the characteristic frequency, F_{HF}, at which the impedance diagram in the Nyquist plot intercepts the real axis (Fig. 2 indicates the meaning of R_{HF} and F_{HF}). To determine F_{HF} it is then clear that the electrochemical impedance of the system must be previously measured before performing the real-time measurements of R_{HF} and V.

The voltage response of the battery cell was processed in two independent channels. In the V measurement channel, the sinusoidal component at frequency F_{HF} was eliminated by a low-pass filter and the dc-voltage was measured. In the R_{HF} measurement channel, the dc level was eliminated by high-pass filters and the high-frequency component, whose amplitude was proportional to R_{HF}, was amplified, rectified by a diode and low-pass filtered, which gave an analog signal proportional to the instantaneous value of R_{HF}. A detailed description of this device can be found in [21]. The signals at the outputs of the two measurement channels were digitized and processed with a real-time computer (Concurrent Computer RTU 6600).

Tests were carried out with a home-made specific galvanostat that allowed simultaneous charging (or discharging) of the 1200 Ah LAB cell and electrochemical measurements. Real-time evolutions of both R_{HF} and V could then be simultaneously measured during charge and discharge cycles. The maximum dc current provided by the galvanostat was 10 A, which limited charging and discharging at the maximum rate of C/120. The values of R_{HF} in the mΩ range required current perturbations of very large amplitude

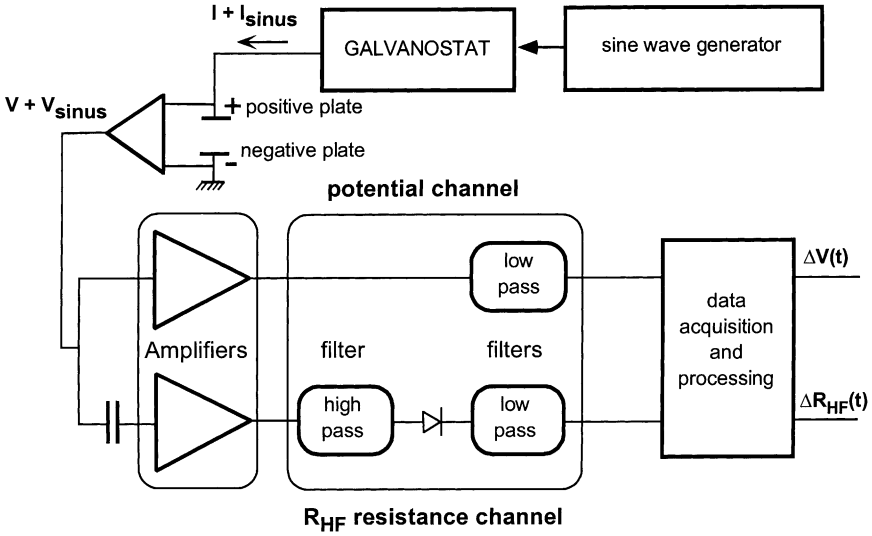

Fig. 1. Experimental set-up for the real-time measurement of V and R_{HF}.

(e.g. 10 A for a R_{HF} value in the range 0.5–1 mΩ to get a voltage response amplitude between 5 and 10 mV) superimposed on the charging or discharging dc current that was also delivered by the galvanostat.

On the other hand, the overall electrode impedance, Z_T, was measured between the positive and negative plates by using a white noise as excitation signal. In addition, the use of a reference electrode (mercureous sulfate electrode) immersed in the acid bath above the plates, allowed the potentials, V_{pos} and V_{neg}, of the positive and negative plates to be measured separately. This also allowed the electrochemical impedances, Z_{pos} and Z_{neg}, of the positive and negative plates to be measured. All experiments were carried out at room temperature.

3. Results and discussion

Because of the very weak impedance values involved, special care has been taken in devising the specific measuring device and also in the choice of the cables and connectors used in the R_{HF} measurement, since bad connections can lead to strongly biased R_{HF} values. This measurement difficulty may possibly account for the divergent results obtained in field tests performed with portable conductance measuring devices. For example, Fig. 2 shows several electrochemical impedance diagrams of a 45 Ah LAB cell obtained with different connectors. These measurements, performed on the same cell at a zero current, show a large scattering of R_{HF} values associated with bad connections to the battery terminals. The diagrams were considered valid when the overall cell impedance, Z_T, was equal to the sum of Z_{pos} and Z_{neg}, measured independently with the help of the reference electrode, at all frequencies analyzed [22]. This criterion, illustrated in Fig. 3, has been extensively employed in this work to fix the connection problems before investigating the time evolutions of R_{HF} and V.

Another important parameter to consider are the charge and discharge rates and their influence on the R_{HF} values. Because of limitations on the galvanostat used to perform electrochemical measurements, which delivered a maximum dc current of 10 A, the 1200 Ah LAB charge and discharge rates were limited to C/120 and no information could be obtained on the R_{HF} changes under faster cycling. This was not a serious drawback since the discharge rates of photovoltaic LAB are in practice performed at smaller current values. For this reason, a set of impedance measurements was carried out on 45 Ah LAB cells (2 V, CEAC-Exide, tubular technology) at different rates between C/10 and C/100. Fig. 4 illustrates the typical high-frequency ($f > 1$ Hz) features of the electrochemical impedance of the cell in rest conditions ($I = 0$) after a full charge, and after a full discharge at two discharge rates. It can be seen that the wider range of R_{HF} variations was obtained at slow discharge rates (160% of the initial value at C/100, 50% at C/10). This clearly indicates that the R_{HF} changes depend on the profile of charge and discharge used, which can be related to the rate of growth or dissolution of insulating $PbSO_4$ crystals as discussed below.

Typical impedance diagrams of the 1200 Ah LAB cell and of the positive and negative plates at rest are shown in Fig. 5. They all strongly depend on SOC in the whole frequency range, with higher R_{HF} values at low SOC, as for the 45 Ah LAB cell (Fig. 4). The differences in R_{HF} values between charged and discharged conditions were about 600 μΩ for the cell, 200 μΩ for the negative plate and 400 μΩ for the positive plate. These low differences illustrate how crucial is the connection problem if it is considered that impedance curves separated by a resistance of 10 mΩ due to inappropriate connection procedures are exhibited in Fig. 2. The very good agreement between Z_T and $Z_{pos} + Z_{neg}$ shown in Fig. 3 indicates that reliable electrochemical impedance and R_{HF} measurements have been performed in this work, even in this very low range of impedance values.

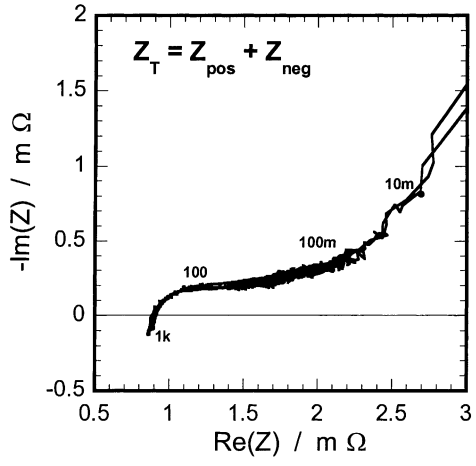

Fig. 3. Comparison of the impedance Z_T of a 1200 Ah LAB cell at rest after a full discharge at a C/120 rate with the sum $Z_{pos} + Z_{neg}$ of the impedances of the positive and negative plates (frequencies in Hz).

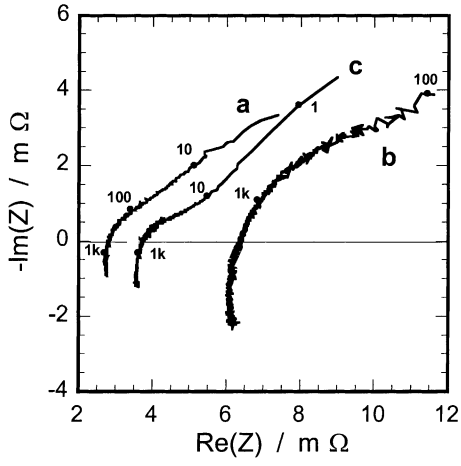

Fig. 4. Nyquist diagrams of the impedance of a 45 Ah LAB cell at rest after (a) a full charge; (b) a full discharge at a C/100 rate; (c) a full discharge at a C/10 rate (frequencies in Hz).

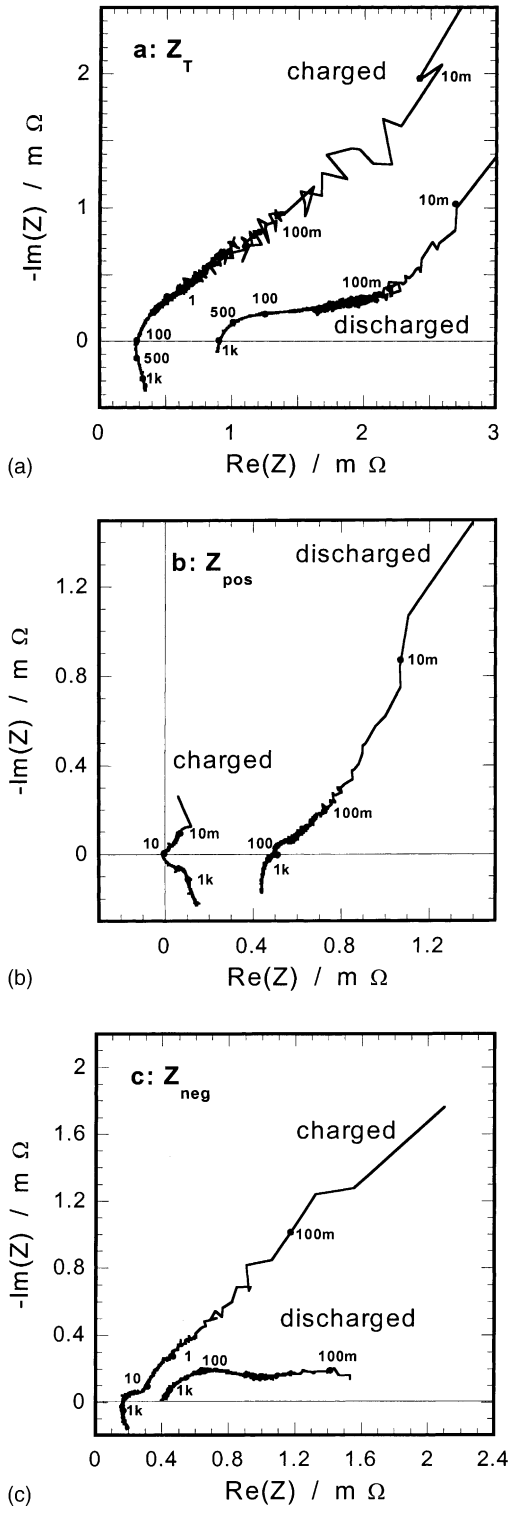

Fig. 5. Nyquist diagrams of the impedances (a) Z_T between the terminals, (b) Z_{pos} of the positive plate, (c) Z_{neg} of the negative plate of a 1200 Ah LAB cell at rest after a full charge at a C/120 rate, and after a full discharge at a C/120 rate (frequencies in Hz).

The general behavior of the electrochemical impedance in charged and discharged conditions is a well-known characteristic of LAB [1,3]. Nevertheless, little information about the actual profile of impedance evolution during charge or discharge can be brought up by these impedance measurements at low and high SOC. On the contrary, real-time measurements of V and R_{HF} during the charge and discharge of the cell allow the simultaneous time evolution of these quantities to be assessed as a function of SOC.

As discussed above, reliable real-time measurements of R_{HF} depend on the previous knowledge of the characteristic frequency F_{HF}. Fig. 5a shows that the F_{HF} values depend on SOC, as well as R_{HF}. The frequency of the perturbation signal used in the R_{HF} measurement was then chosen after preliminary impedance measurements during complete charge/discharge cycles of the cell at a C/120 rate. The values of F_{HF}, $F_{HF,pos}$, $F_{HF,neg}$ and the corresponding values R_{HF} of Z_T, $R_{HF,pos}$ of Z_{pos}, $R_{HF,neg}$ of Z_{neg} were measured at various SOC in rest conditions. The limiting values for each cycle, given in Fig. 6a and b, show a good reproducibility in the R_{HF} values and a significant dispersion in the F_{HF} values. For the impedance Z_T measured at the terminals of the cell, R_{HF} varied from 0.2 mΩ for a fully charged cell to 1 mΩ for a fully discharged cell and F_{HF} varied from 100 Hz to 1 kHz, respectively. For the positive plate, Fig. 6a exhibits slightly negative values of $R_{HF,pos}$. They were due to limitations in the instrumentation used for very small impedance values (a few tens of μΩ). Furthermore, Fig. 6a shows that R_{HF} was not equal to $R_{HF,pos} + R_{HF,neg}$ for the fully charged cell, while Z_T was actually equal to $Z_{pos} + Z_{neg}$ at each frequency. This comes from the fact that the frequencies F_{HF}, $F_{HF,pos}$ and $F_{HF,neg}$ corresponding to R_{HF}, $R_{HF,pos}$, and $R_{HF,neg}$ had different values, as shown in Fig. 6b. For the fully discharged cell, R_{HF} was close to $R_{HF,pos} + R_{HF,neg}$ despite the difference in F_{HF} values.

It must be realized that the experimental set-up allowed real-time measurements of the modulus, not the real part, of the impedance of the cell at the perturbation frequency. So, to minimize the measurement error on R_{HF} due to the progressive change in F_{HF} with SOC, an intermediate value of 500 Hz was taken for the perturbation frequency. It can be seen in Fig. 5a that the modulus of the impedance at 500 Hz is actually close to R_{HF} both in the charged and discharged conditions.

Fig. 7 presents the typical evolution of R_{HF}, V, V_{neg}, and V_{pos} during a 1200 Ah cell discharge at C/120. The end of the discharge was due to the negative plate exhaustion, as shown by the sharp V_{neg} drop before current interruption. R_{HF} changed very little during the first part of the discharge, then it increased, following the progressive screening of the plate surface by insulating $PbSO_4$ deposits. Beyond 75% of the total supplied charge, R_{HF} increased rapidly till the end of the discharge. This behavior was related to the screening of the last accessible areas of active mass by $PbSO_4$ crystals, or to an increase in resistivity of the electrolyte in the pores of the active mass since the ionic concentration is strongly reduced there at the end of the discharge. After the current break, the relaxation of R_{HF} exhibited in Fig. 7, from 1.7 mΩ towards 1.0 mΩ, the value of R_{HF} at low SOC given in Fig. 6a, might be associated to the redissolution of the $PbSO_4$

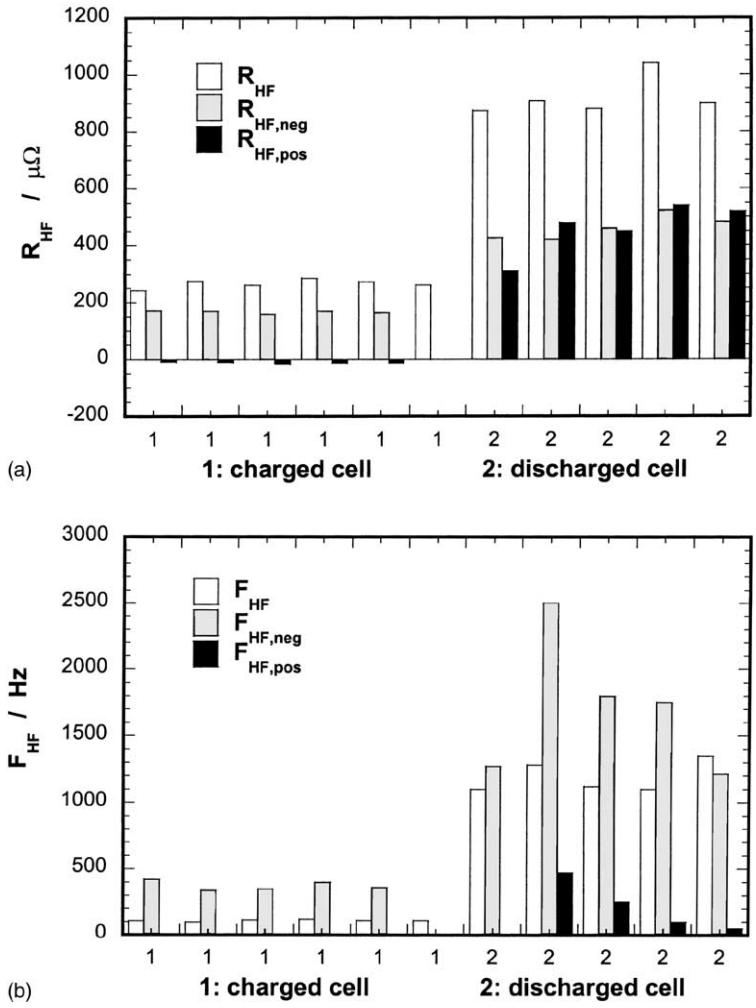

Fig. 6. Values of (a) R_{HF} and (b) F_{HF} for a 1200 Ah LAB cell at rest, its positive plate, and its negative plate, after a full charge at a C/120 rate, and after a full discharge at a C/120 rate.

crystals formed locally at high current densities at the end of the discharge, or to the increase in the concentration of ions diffusing back from the electrolyte bulk towards the pores of the active mass.

Fig. 8 shows the time evolution of R_{HF}, V, V_{neg}, and V_{pos} during three charges of the 1200 Ah cell. For each quantity, the three curves were essentially identical; the shift towards lower applied charge to obtain a battery voltage of 2.4 V was

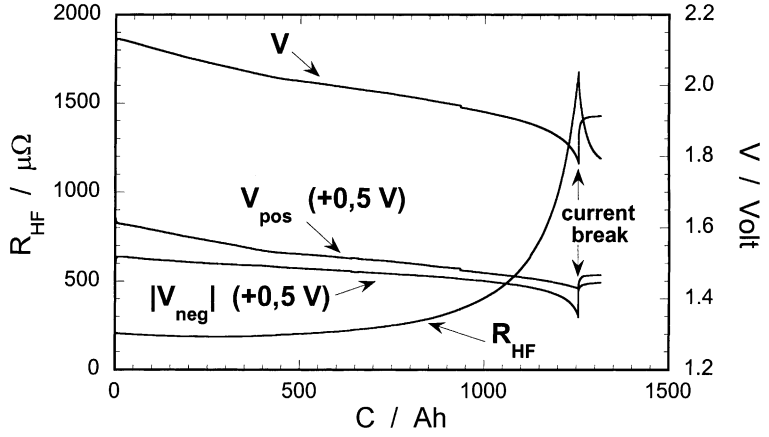

Fig. 7. Evolution of R_{HF}, V, V_{pos}, V_{neg} during the discharge of a 1200 Ah LAB cell at a C/120 rate as a function of the charge delivered. The potentials of the positive and negative plates have been shifted vertically by 0.5 V.

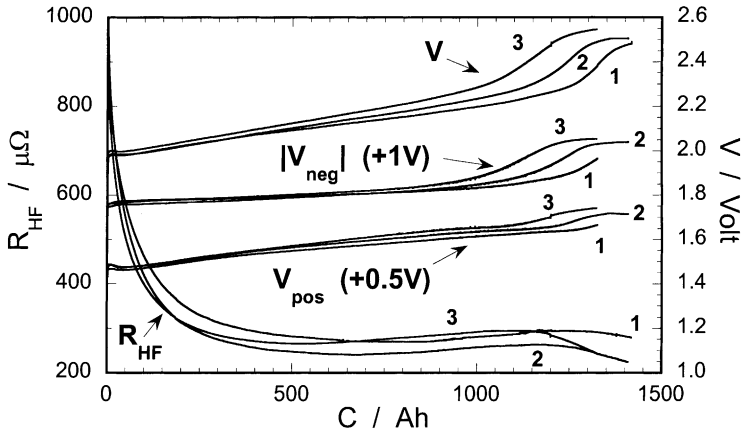

Fig. 8. Evolution of R_{HF}, V, V_{pos}, V_{neg} during the charge of a 1200 Ah LAB cell at a C/120 rate as a function of the charge supplied. The potentials of the positive and negative plates have been shifted vertically by 0.5 and 1 V, respectively.

explained by an incomplete discharge at 1.8 V, where the current was switched off, before each charge. R_{HF} decreased quickly in the first part of the charge (up to 25% discharge) because of rapid dissolution of unstable $PbSO_4$ crystals formed at high local current density at the last stage of the preceding discharge. In the second half of the charge R_{HF} slightly increased, and then finally decreased again. The slow increase seems to be related to the progressive appearance of H_2 bubbles locally blocking the active mass. As the charge went on, dissolved hydrogen production became more and more important and the forced convection caused by gas evolution yielded fast bubble ejection. As a consequence, the mean lifetime of bubbles over the active mass surface became smaller, which probably explained the R_{HF} decrease.

Concerning the possible causes of R_{HF} changes during the charge or discharge of LAB, Figs. 3 and 6a provide a first evidence that they cannot be fully ascribed to changes in the electrolyte resistivity, ρ, of the acid bath. Indeed, $R_{HF,pos}$ and $R_{HF,neg}$, measured between the reference electrode and the positive and negative plate, respectively, include the contribution due to the resistivity of the electrolyte above the plates where the reference electrode was positioned. Since R_{HF} of the fully discharged cell, measured between the plates, was equal to $R_{HF,pos} + R_{HF,neg}$, the contribution of the electrolyte resistivity can be neglected. Nevertheless, specific experiments have been performed to further investigate the dependence of R_{HF} on ρ. A first test, carried out on a LAB cell of 45 Ah, consisted in replacing the exhausted electrolyte by fresh solution after a complete discharge, which gave no significant change in R_{HF} that also remained constant after refilling the battery with the previously exhausted acid. This was another clear evidence that R_{HF} did not explicitly depend on the bulk electrolyte resistivity. In subsequent experiments, the electrolyte resistivity was measured during the charge or discharge of the LAB by immersing a conductivity cell above the plates. Fig. 9 shows the comparative behavior of R_{HF} and ρ during the charge of

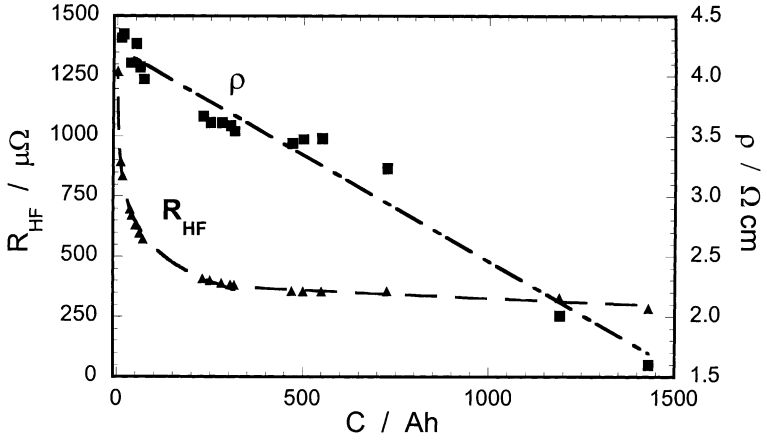

Fig. 9. Evolution of R_{HF} and ρ during the charge of a 1200 Ah LAB cell at a C/120 rate as a function of the charge supplied.

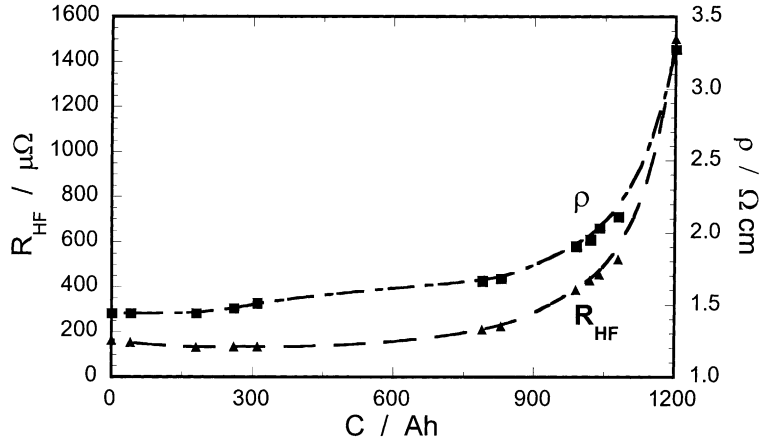

Fig. 10. Evolution of R_{HF} and ρ during the discharge of a 1200 Ah LAB cell at a C/120 rate as a function of the charge delivered.

the 1200 Ah cell. It is worth noticing that ρ was measured above the plates and not at the actual reactive plates/electrolyte interface. During the charge, the ionic concentration increase at the interface was rapidly picked up above the plates so that ρ decreased, approximately linearly, during the whole charge, in contrast with the R_{HF} behavior. This fast mass transport between the interface and the electrolyte bulk was due to the forced convection induced by hydrogen bubble evolution that took place since the beginning of the charge, as shown by noise measurements that will be the matter of a future publication.

A quite different behavior was observed during the discharge of the 1200 Ah cell where R_{HF} and ρ increased in the same way (Fig. 10). However, this cannot be taken as an evidence of a straightforward relationship between these two quantities. In the case of battery discharge, no hydrogen bubble evolution takes place and mass transport is ensured by diffusion only. Hence, the decrease in ionic concentration in the pores of the active mass did not instantly modify the resistivity of the bulk electrolyte, which remained almost constant until about 75% of the discharge. At the end of the discharge, the acid bath was almost completely exhausted and, therefore, ρ increased.

The above results show that R_{HF} effectively depends on SOC. The main feature of the time evolution profile was that most of the R_{HF} variations took place at the first stage of the charge and at the end of the discharge of the LAB cell. During about 75% of both charge and discharge, R_{HF} showed a slow drift preceded (charge) or followed (discharge) by an abrupt inflection of the curve. As a consequence, the SOC monitoring by means of the R_{HF} values remains a difficult task mainly in practical conditions where the charges and discharges are often irregular or incomplete. However, it seems that R_{HF} measurements could effectively be used as an indicator of the last stage of the discharge to inform that only a small charge is available.

Another interesting result obtained in this study concerns the relationship between the R_{HF} values and the SOH of LAB cells. Over-discharged or aged batteries presented a shorter range of R_{HF} variations that seemed to indicate a gradual loss of efficiency in the charge/discharge cycles, since the total charge delivered by those cells was smaller after aging. This can be seen as a possible indication that a SOH diagnostics could be based on R_{HF} measurements.

4. Conclusions

It has been shown in this work that the high-frequency resistance of a 1200 Ah LAB cell used in photovoltaic applications is directly dependent on SOC in a non-linear way. Moreover, experiments carried out with 45 Ah LAB cells at various charge/discharge rates (C/10 to C/100) yielded different R_{HF} evolution profiles and different ranges of R_{HF} variations. Hence, monitoring the SOC from the single R_{HF} value seems difficult in practical conditions where the charge/discharge rate varies with time. Nevertheless, it seems to be possible to devise an end-of-discharge or low-charge alarm based on R_{HF} measurements, mainly in applications with typical low rate discharge profile. On the other hand, monitoring R_{HF} for batteries in operating conditions should also give a deeper insight into the SOH of the batteries.

The R_{HF} changes cannot be ascribed to the variations in resistivity of the bulk electrolyte. The blocking action of insulating $PbSO_4$ crystals in the pores of the active mass is instantaneously reflected in the R_{HF} value and represents the main component of the R_{HF} variations during the charge and discharge of LAB. This component strongly depends on the (dis)charge rate because this parameter controls the shape and size of the $PbSO_4$ crystals.

Acknowledgements

The authors would like to acknowledge the financial support of CEAC and ADEME (convention no. 99-05-081).

References

[1] F. Huet, J. Power Sources 70 (1998) 59–69 (and references therein).
[2] S. Rodrigues, N. Munichandraiah, A.K. Shukla, J. Power Sources 87 (2000) 12–20.
[3] N. Yahchouchi, Ph.D. thesis, University Paris 6, France, 1981.
[4] D.O. Feder, T.G. Croda, K.S. Champlin, S.J. McShane, M.J. Hlavac, J. Power Sources 40 (1992) 235–250.
[5] G.J. Markle, in: Proceedings of the INTELEC Conference, Washington, DC, 4–8 October 1992, pp. 212–217.
[6] P. Waltari, T. Suntio, in: Proceedings of the INTELEC Conference, paper 21–2, Copenhagen, Denmark, 6–9 June 1999.
[7] S. Piller, M. Perrin, A. Jossen, J. Power Sources 96 (2001) 113–120.
[8] A.R. Waters, K.R. Bullock, C.S.C. Bose, in: Proceedings of the INTELEC Conference, Melbourne, Australia, 19–23 October 1997, pp. 675–680.
[9] W.H. Edwards, A.I. Harrison, T.M. Wolstenholme, in: Proceedings of the INTELEC Conference, paper 18–3, Copenhagen, Denmark, 6–9 June 1999.
[10] M. Kniveton, A.I. Harrison, in: Proceedings of the INTELEC Conference, San Francisco, CA, 4–8 October 1998, pp. 695–702.
[11] A.K. Shukla, V. Ganesh Kumar, N. Munichandraiah, T.S. Srinath, J. Power Sources 74 (1998) 234–239.
[12] Z. Noworolski, U. Reskov, in: Proceedings of the INTELEC Conference, San Francisco, CA, 4–8 October 1998, pp. 215–220.
[13] E. Karden, S. Buller, R.W. De Doncker, J. Power Sources 85 (2000) 72–78.
[14] D.O. Feder, M.J. Hlavac, W. Koster, J. Power Sources 46 (1993) 391–415.
[15] M. Kim, E. Hwang, J. Power Sources 64 (1997) 193–196.
[16] I. Kurisawa, M. Iwata, in: Proceedings of the INTELEC Conference, Melbourne, Australia, 19–23 October 1997, pp. 687–694.
[17] M. Calábek, K. Micka, P. Baca, P. Krivack, V. Smarda, J. Power Sources 62 (1996) 161–166.
[18] M. Calábek, K. Micka, P. Baca, P. Krivack, V. Smarda, J. Power Sources 64 (1997) 123–129.
[19] T. Takasaki, K. Takano, M. Ichimura, in: Proceedings of the INTELEC Conference, Boston, MA, 6–10 October 1996, pp. 799–804.
[20] K. Kozuka, K. Takano, Y. Konya, Y. Kawagoe, in: Proceedings of the INTELEC Conference, Melbourne, Australia, 19–23 October 1997, pp. 397–402.
[21] C. Gabrielli, F. Huet, M. Keddam, J. Electrochem. Soc. 138 (1991) L82–L84.
[22] M. Keddam, Z. Stoynov, H. Takenouti, J. Appl. Electrochem. 7 (1977) 539–544.